

**Revisiting the role of CFTR and counterion permeability in the pH  
regulation of endocytic organelles**

Herve Barriere<sup>1</sup>, Miklos Bagdany<sup>1</sup>, Florian Bossard<sup>1</sup>, Tsukasa Okiyonedo<sup>1</sup>, Gabriella  
Wojewodka<sup>2</sup>, Dieter Gruenert<sup>3</sup> Danuta Radzioch<sup>2</sup> and Gergely L. Lukacs<sup>1,\*</sup>

**Supplemental materials**

## ***Supplemental Methods***

### **Metabolic pulse chase analysis**

The wt and G551D CFTR maturation efficiency was measured by the pulse chase technique essentially as described (Du *et al.*, 2005). Briefly, CFTR expressing BHK cells expressing were pulse-labeled with 0.1 mCi/ml of Easy Tag Express Protein Labeling Mix (Perkin Elmer) for 20 min and chased for the indicated time at 37°C with DMEM/F12 medium supplemented with 5% FBS and 2 mM of cysteine and methionine. CFTR was solubilized in RIPA buffer (150 mM NaCl, 20 mM Tris-HCl, 1% (w/v) Triton X-100, 0.1% (w/v) SDS and 0.5% (w/v) sodium deoxycholate, pH 8.0) supplemented with protease inhibitors (10 µg/ml leupeptin and pepstatin, 1 mM PMSF) and immunoprecipitated with monoclonal M3A7 and L12B4 anti-CFTR antibodies. The radioactivity associated with CFTR was visualized by SDS-PAGE and fluorography and quantified using a Typhoon workstation with the ImageQuant TL software (GE Healthcare).

### **Electrophysiology**

Currents were recorded in whole-cell configuration using an Axopatch 200B amplifier and Digidata 1440A data acquisition hardware (Molecular Devices Inc., Union City, CA, USA). The pipette filling solution contained (in mM) 110 Na-gluconate, 20 NaCl, 8 MgCl<sub>2</sub>, 5 EGTA, 10 glucose, 2 ATP, and 10 HEPES, pH 7.2. The bath solution was as follows: 137 NaCl, 3 MgCl<sub>2</sub>, 1 CaCl<sub>2</sub>, 10 glucose, 10 HEPES, pH 7.2. In antibody-binding experiments cells were pre-incubated for 30 min at room temperature with anti-HA (1:500 dilution, 10 µg/ml MMS101R, Covance) primary Ab. Channels were activated by 20 µM forskolin, 0.2 mM IBMX, and 0.5 mM CTP-cAMP adding to the bath solution. The membrane potential was held at -60 mV. For analysis of the current-voltage relationship, the potential was stepped from -90 mV to +90 mV for 300 ms in 15 mV increments. For data acquisition and analysis, the pClamp-10 software package (Molecular Devices Inc., Union City, CA, USA) was used. Currents were normalized for the cell capacitance to eliminate variations in cell size. All electrophysiological measurements were conducted at room temperature (22–24 °C).

### **Colocalization analysis**

Colocalization was performed using “Colocalization” feature in the Volocity 4.1.0 (Molecular Devices) software. The background fluorescence was defined on mock transfected or non-labeled cells and subtracted in manually defined regions of interest in both green and red channels. Manders' overlap coefficient, provided by the Volocity 4.1.0 software, is based on the Pearson's correlation coefficient with average intensity values being taken out of the mathematical expression as described in (Manders *et al.*, 1992). This coefficient represents the fraction of the total green fluorescence that overlapped with the red channel and *vice versa*. The values are then expressed as percentage of colocalization.

## ***Supplemental Figure Legends***

**Supplemental Figure 1.** (A) Anti-HA and anti-mouse IgG pH-sensitive dissociation from CFTR-3HA. To confirm that the primary and secondary Ab remains bound to CFTR during FRIA experiments, the antibody complex binding to the cell surface wt CFTR-3HA was determined at the indicated pH as described in Methods. (B) *In situ* pH calibration curve of phagosomes and endosomes of CFTR expressing RAW cells, labeled with FITC-conjugated *P. aeruginosa* and anti-HA+FITC-Fab complex, respectively. The organelles pH was clamped between pH 4.0 and 8.0 in K<sup>+</sup>-rich medium (135 mM KCl, 10 mM NaCl, 20 mM Hepes or 20 mM MES, 1 mM MgCl<sub>2</sub>, and 0.1 mM CaCl<sub>2</sub>) with 10 μM nigericin, 10 μM monensin, 400 nM Baf and 20 μM CCCP (Sigma-Aldrich, Oakville, ON, Canada) and FRIA was performed as described in Methods. Similar calibration curves were obtained in other cell lines (data not shown). (C-D) *In situ* pH calibration curve of FITC-TMR-dextran labeled lysosomes and phagosomes ingested FITC and TRITC labeled *P. aeruginosa* in primary peritoneal mouse macrophages. FRIA was performed at 490 nm with 540 nm excitation wavelengths after clamping the lysosomal and phagosomal pH as above.

**Supplemental Figure 2.** (A) Plasma membrane density of wt and G551D CFTR-3HA in BHK, IB3, CFBE, HeLa and MDCK cells. CFTR density was measured by immunoperoxidase assay, using anti-HA primary (MMS101R, Covance, 0°C, 1 h) and horseradish peroxidase (HRP)-conjugated goat anti-mouse secondary antibody (Amersham Biosciences, 0° C, 1 h) in PBS supplemented with 0.1 mM CaCl<sub>2</sub>, 1 mM MgCl<sub>2</sub> (PBS/C-M) and 0.5% BSA. The Amplex Red fluorescence signal was detected by fluorescence plate reader as described (Barriere *et al.*, 2006). Specific binding was calculated by subtracting the non-specific signal in the presence of 10 mg/ml non-immune IgG (Santa Cruz Biotechnology Inc.) and the secondary antibody. The signal was normalized for the cellular protein concentration. Means ± SEM, n= 3. (B) Folding efficiency of wt- and G551D-CFTR. BHK cells expressing wt or G551D-CFTR-3HA were pulse-labeled for 20 min then chased for 3 hours. CFTR was immunoprecipitated with M3A7 and L12B4 anti-CFTR antibodies and analyzed by SDS-PAGE and fluorography. The radioactivity was quantified using a Typhoon workstation with the ImageQuant TL software

(GE Healthcare). Means  $\pm$  SEM, n= 4. (C) Metabolic stability of the mature, complex-glycosylated wt- and G551D-CFTR was measured by pulse-chase experiments after pulse-labeling for 20 min and chasing for 3 h to allow complete maturation of the labeled CFTR pool (t=0). Following the additional chase (0-36 h), the remaining CFTR radioactivity was quantified by phosphorimaging analysis and expressed as percentage of the initial value. Means  $\pm$  SEM, n = 3.

**Supplemental Figure 3.** Intracellular distribution and function of wt and G551D CFTR.

(A) Colocalization of internalized CFTR and Tf-R. CFTR and Tf-R were labeled as in Figure 1D in BHK cells and single optical sections were obtained by fluorescence laser confocal microscopy. Black bar: TMR-Tf loaded cells were chased 2-5 min; white bar, cells were visualized without chase. The colocalization analyses were performed using Volocity software (Molecular Device) as described in Supplementary material and Methods. Tf-R/wt or TfR/G551D colocalization represents the percentage of Tf-R fluorescence overlap with that of the CFTR. wt/TfR and G551D/TfR indicate the percentage of CFTR colocalization with the Tf-R. Means  $\pm$  SEM are based on 10 different fields, each containing 10-15 cells. (B) Internalized wt CFTR colocalizes with EEA1 and Rab5 but only marginally with Rab9 in BHK cells. CFTR-3HA was labeled with anti-HA antibody for 1 h and chased for 0.5 h prior to fixation, permeabilization and visualization with TRITC-conjugated goat anti-mouse Fab. EEA1 and Rab5 were detected by indirect immunostaining using rabbit polyclonal anti-EEA1 antibody from Abcam Ltd (Cambridge, UK) and anti-Rab5 Ab from Santa Cruz Biotechnology, (Santa Cruz, CA). Rab9 was detected by indirect immunostaining using the monoclonal mouse anti-Rab9 antibody (Cedarlane, Canada) and goat anti-mouse IgG (Jackson ImmunoResearch, CA). Single optical sections were obtained by a Zeiss LSM510 laser confocal fluorescence microscope as described in *Methods*. Bar: 10  $\mu$ m. (C) Localization of internalized wt and G551D CFTR with recycling endosomes and lysosomes in HeLa cells. Internalized CFTR was labeled as described in *panel B*. Recycling endosomes and lysosomes were visualized by FITC-Tf and FITC-dextran loading, respectively, as described in *Methods*. Bar: 10  $\mu$ m. (D) Quantitative colocalization of internalized CFTR with the indicated marker on micrographs obtained as shown in *panels B* and *C*. Colocalization was analysed as in *panel A*. (E) The pH dissipation rate of Tf-FITC containing vesicles in wt or G551D CFTR expressing cell lines was measured using

the rapid pH dissipation method as described in Figure 2E. FITC-Tf loading was described in the Methods.

**Supplemental Figure 4.** (A) The anti-HA Ab binding effect on the CFTR-3HA channel activity. The plasma membrane conductance of CFTR-3HA expressing BHK cells was measured in whole-cell configuration as described in *Methods* before and after stimulation with PKA agonist cocktail (20  $\mu$ M forskolin (FK), 0.2 mM IBMX, and 0.5 mM CPT-cAMP). When indicated, anti-HA Ab at identical concentration that was used to label the endosomal compartment was bound to the BHK cells for 30 min at room temperature. CFTR current-voltage relationships were determined before and after PKA stimulation (+FK) in the control and anti-HA Ab exposed (+Ab) cells. (B) The CFTR current density development was plotted as a function of time in control and anti-HA Ab (+Ab) treated cells at +75 mV of holding membrane potential. The current values were normalized for the cellular capacitance. Means  $\pm$  SEM; n = 9

**Supplemental Figure 5.** The pH-sensitivity of the CFTR chloride channel activity at the plasma membrane. Wt CFTR activity was measured by the iodide efflux assay as described in Figure 1C at 22°C. Iodide efflux was stimulated by PKA agonist cocktail or by 10  $\mu$ M Ca<sup>2+</sup> ionophore A23187 to activate Ca<sup>2+</sup>-activated Cl<sup>-</sup> channels. Cells were incubated during the last 10 min of the iodide loading and during the efflux measurements in pH=5 MES buffered medium as indicated in Methods. The electrode was calibrated in medium with pH=5. Data are means of triplicate determinations from a representative experiment of three.

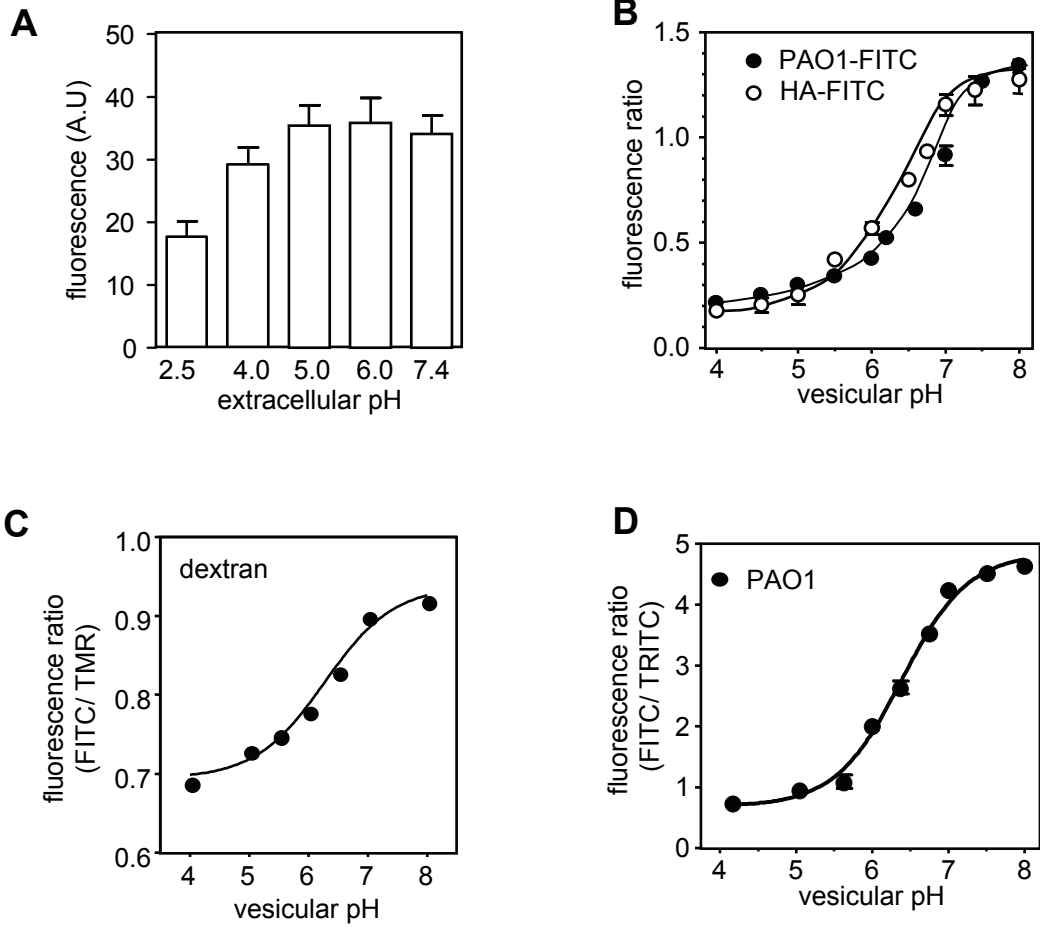
**Supplemental Figure 6.** CFTR ablation and overexpression has no effect on the pH regulation of lysosomes. (A) CFTR knockdown and PKA activation has no effect on the lysosomal pH in primary alveolar and peritoneal macrophages isolated from *cftr* +/+ and -/- mice, respectively. Lysosomes were loaded with FITC-dextran or Oregon488-dextran (50  $\mu$ g/ml, M.W.:10 kDa, Molecular Probes, Inc.) overnight and chased for >3 hours at 37°C to ensure that the dye is exclusively associated with lysosomes (Kumar *et al.*, 2007). Lysosomal pH was measured by FRIA before and after PKA agonist cocktail (FK; 20  $\mu$ M forskolin, 0.5 mM CPT-cAMP and 0.2 mM IBMX) addition for 3 min. Means  $\pm$  SEM; n = 4 mice. (B) and (C) The effect of

CFTR complementation of CF respiratory epithelia (CFBE and IB3) and CFTR overexpression in BHK and HeLa cells on the counterion conductance and steady-state pH of lysosomes. The lysosomes of parental, wt or G551D CFTR expressing cells were loaded with FITC/Oregon green 488-dextran as described in *panel A*. The CCCP+Baf-induced pH dissipation rate, an indicator of the counter permeability of lysosomes in the absence or presence of PKA activation (+FK), was determined as in Figure 2E. Means  $\pm$  SEM; n = 3–5. (C) The lysosomal pH distribution profile was established by FRIA as in Figure 2E-F before and after 3 min stimulation with the PKA agonist cocktail (+FK).

## References :

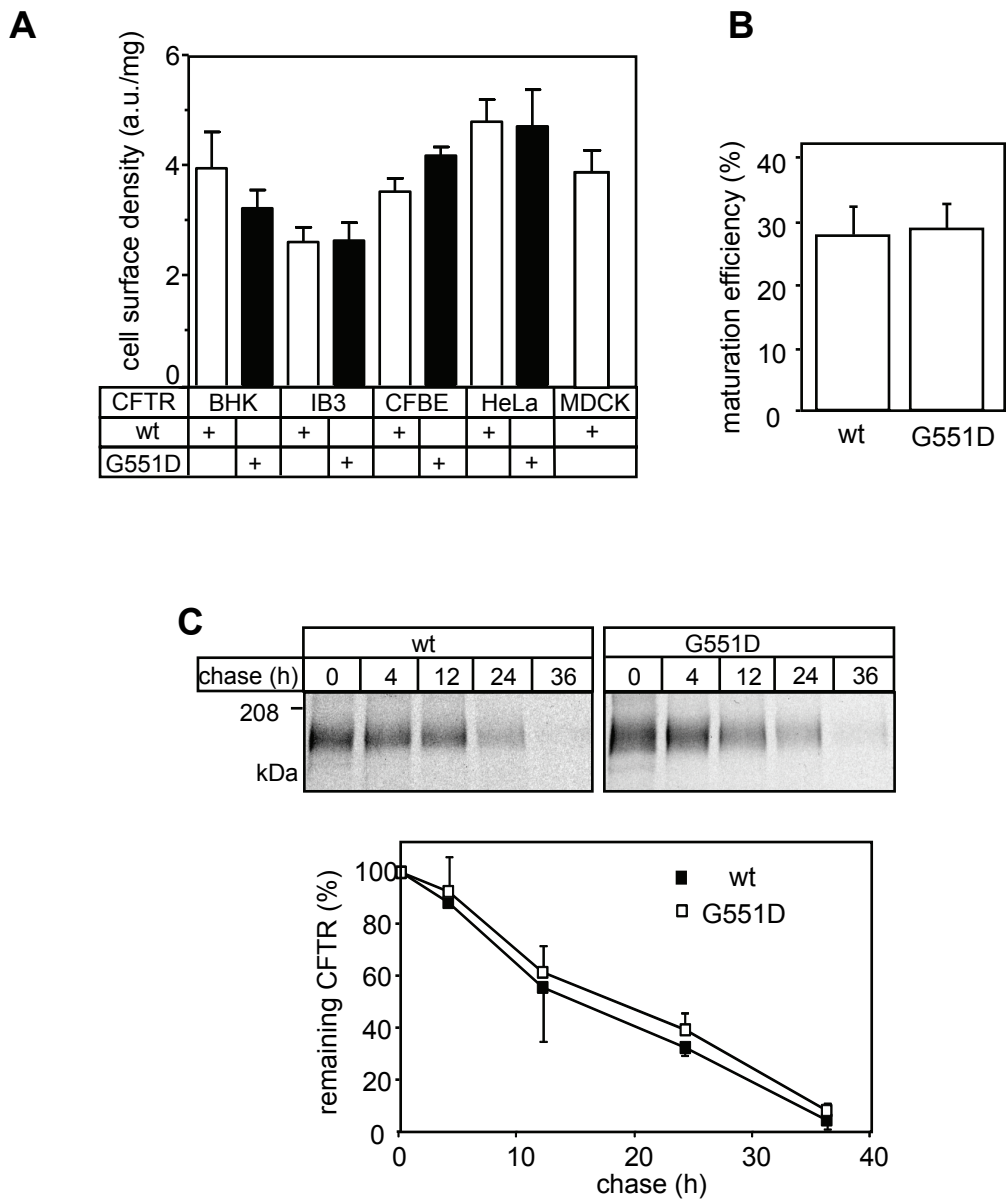
- Barriere, H., Nemes, C., Lechardeur, D., Khan-Mohammad, M., Fruh, K., and Lukacs, G.L. (2006). Molecular basis of oligoubiquitin-dependent internalization of membrane proteins in Mammalian cells. *Traffic* 7, 282-297.
- Du, K., Sharma, M., and Lukacs, G.L. (2005). The DeltaF508 cystic fibrosis mutation impairs domain-domain interactions and arrests post-translational folding of CFTR. *Nat Struct Mol Biol* 12, 17-25.
- Kumar, K.G., Barriere, H., Carbone, C.J., Liu, J., Swaminathan, G., Xu, P., Li, Y., Baker, D.P., Peng, J., Lukacs, G.L., and Fuchs, S.Y. (2007). Site-specific ubiquitination exposes a linear motif to promote interferon-alpha receptor endocytosis. *J Cell Biol* 179, 935-950.
- Manders, E.M., Stap, J., Brakenhoff, G.J., van Driel, R., and Aten, J.A. (1992). Dynamics of three-dimensional replication patterns during the S-phase, analysed by double labelling of DNA and confocal microscopy. *J Cell Sci* 103 (Pt 3), 857-862.

Figure S1





**Figure S2**



**Figure S3**

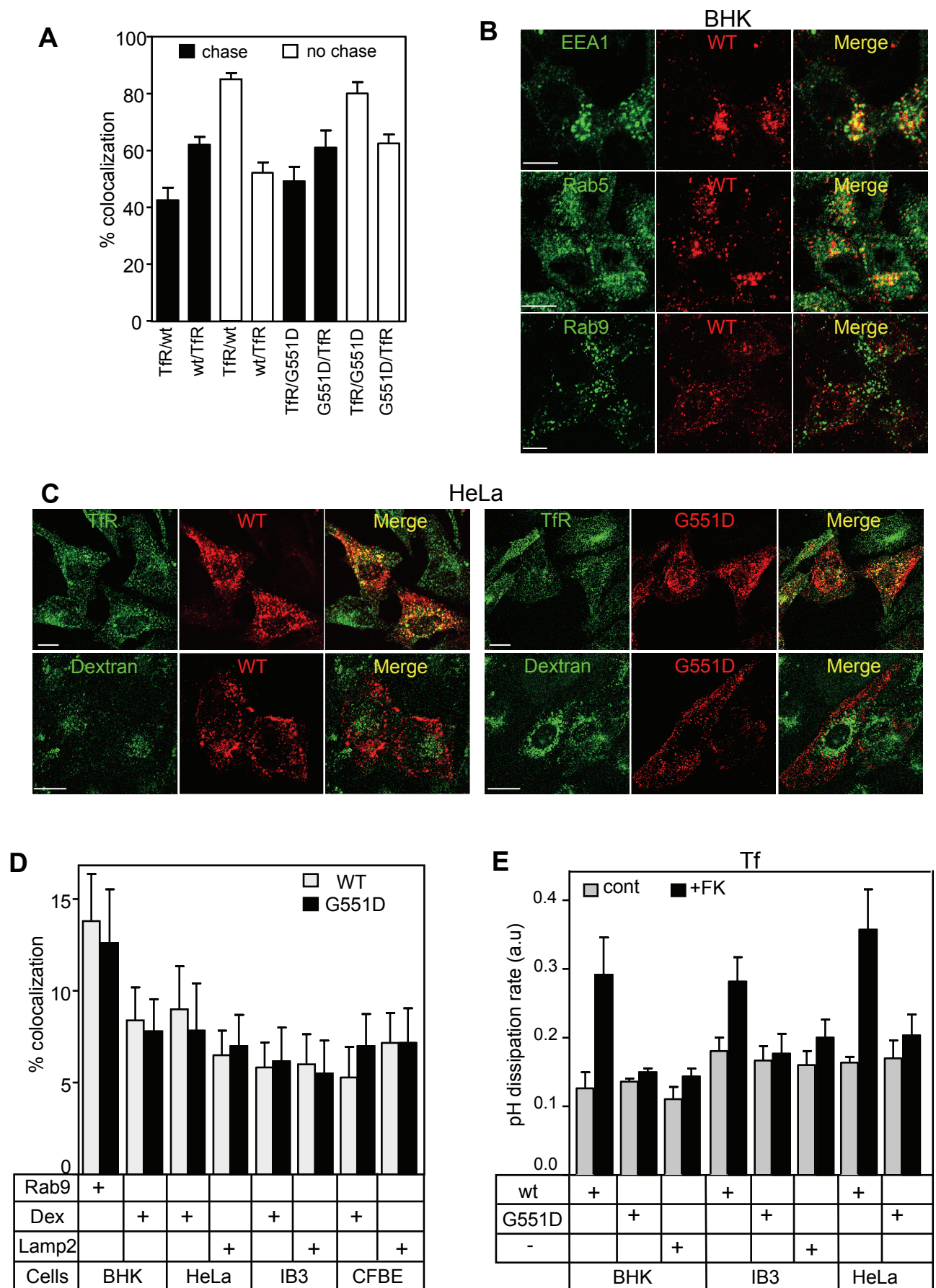
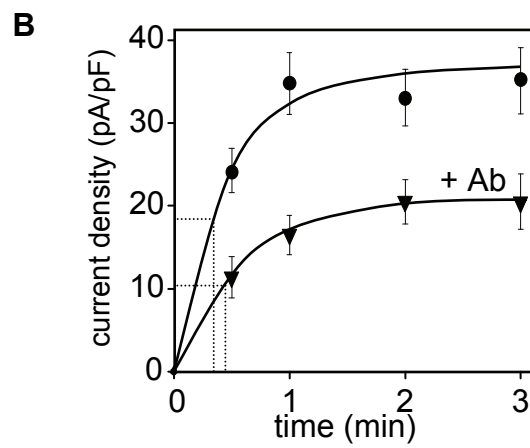
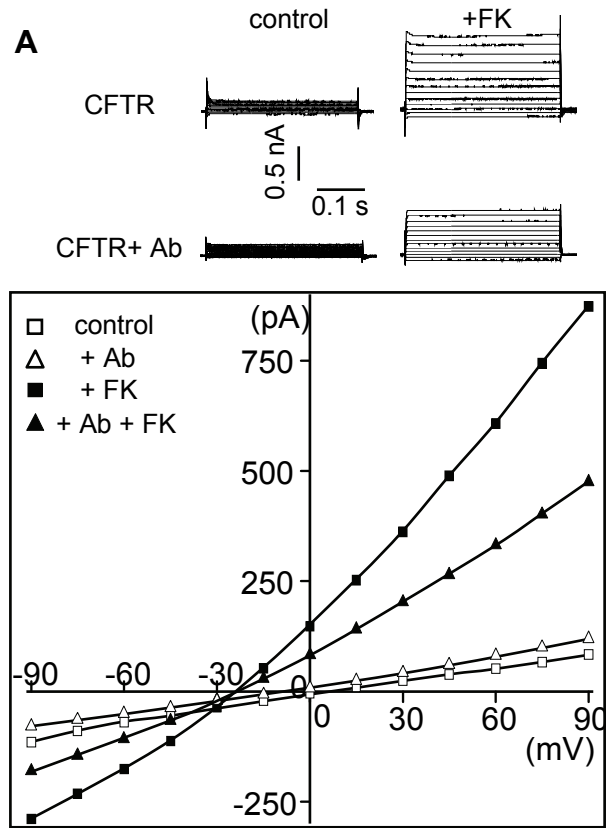


Figure S4



**Figure S5**

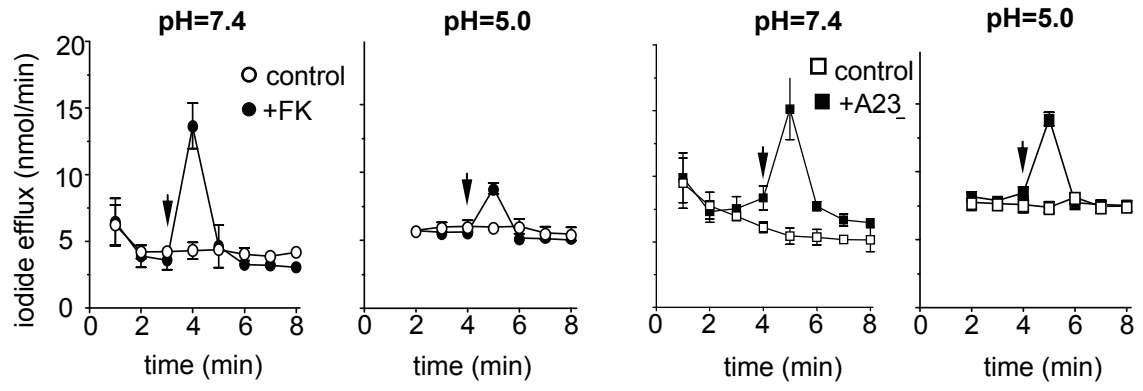


Figure S6

